International Journal of Mathematical, Engineering and Management Sciences
Vol. 11, No. 3, 1444-1464, 2026
https://doi.org/10.33889/IJMEMS.2026.11.3.059

Medical Image Enhancement using Modified HE with DWT and SVD

Anuj Bhardwaj
Department of Mathematics,
Jaypee Institute of Information Technology, 201309, Noida, India.
Corresponding author: anujbhardwaj8@gmail.com

Neha Chandra
Department of Mathematics,
Jaypee Institute of Information Technology, 201309, Noida, India.
E-mail: nehakk305@gmail.com

(Received on December 13, 2025; Revised on March 5, 2026 & April 30, 2026 & May 15, 2025; Accepted on May 20, 2026)

Abstract
Medical imaging is essential for obtaining precise information to assess patient health and provide effective treatment. The initial analysis of a wide range of medical images is vital for identifying abnormalities. However, limitations during the image acquisition process can lead to poor image quality. To address the issues of reduced information and contrast in medical images, the proposed method is designed. The method integrates the spatial frequencies (SF) of both the original image and the image enhanced through Triple Clipped Dynamic Histogram Equalization (TCDHE). Additionally, the discrete wavelet transform and singular value decomposition are applied simultaneously to both images to obtain an improvement factor (gamma), which controls the contrast enhancement rate. The use of spatial frequencies helps preserve the detailed components of an image, such as edges and sharp features. For experimental purposes, three types of datasets are utilized, including MRI, X-ray, and ultrasound. Objective evaluation is performed using seven performance metrics: AMBE, PSNR, SSIM, GMSD, REC, entropy, and subjective evaluation with a mean opinion score. The experimental results demonstrate that AMBE (4.08), SSIM (0.99), PSNR (37.67 dB), and GMSD (0.13) are the best among state-of-the-art methods. However, the results for REC and entropy are comparable to those of state-of-the-art methods. Furthermore, the average values of all performance parameters have been computed across three categories of medical datasets to demonstrate the efficacy of the proposed method.

Keywords- Contrast enhancement, Discrete wavelet transform, Mean opinion score, SVD, Medical image.

1. Introduction

Medical imaging plays a vital role in disease identification, monitoring patient health, and evaluating the effectiveness of treatments. Despite advancements in imaging techniques, the quality of medical images often falls short of the requirements for accurate diagnosis. Various factors contribute to poor image quality, including environmental noise, patient-specific settings, lighting conditions, and limitations of imaging instruments. When an image has uniform and excessive contrast within a narrow range, valuable information can be lost in those areas. Therefore, the challenge lies in improving the contrast of medical images to correctly represent all the information they contain (Dougherty, 2009).

Various techniques have been proposed in the literature to enhance image quality and improve contrast and brightness. Improving the contrast of an image is particularly important for low- or dark-contrast medical images, especially when re-imaging is not feasible. Broadly speaking, contrast enhancement techniques can be categorized into two main classes: frequency domain and spatial domain (Masters et al., 2009). Spatial domain methods involve direct manipulation of pixel values to improve the image, whereas frequency domain methods analyse the rate of change of pixel values, referred to as the image's frequency, using mathematical functions. High-frequency components capture abrupt changes, such as edges, while low-frequency components represent smooth regions in an image.

Histogram Equalization (HE) is a commonly used technique for enhancing image quality. It calculates the histogram of an image and equalizes it to acquire optimal results. However, this method leads to over-enhancement in images due to altered brightness and unwanted artifacts generated in the image. To overcome such limitations, an extended version known as Brightness Preserving Bi-Histogram Equalization (BBHE) was developed (Kim, 1997). In this method, an image is decomposed into sub-images based on its mean value before applying HE. This method aims to retain the overall brightness of the image while improving its visual appearance. There are several other HE-based techniques (Wang et al., 1999; Zuo et al., 2013) and additional spatial domain methods, such as mathematical morphology (Sazak et al., 2019; Wadhwa & Bhardwaj, 2021), adaptive gamma correction (AGC) (Veluchamy & Subramani, 2019; Zhou et al., 2018), and grey level transformation (Gandhamal et al., 2017) for image enhancement. The adaptive fractional differential approach maintains smooth regions in an image while simultaneously enhancing edges and textures. Wadhwa & Bhardwaj (2020) developed a method based on the Grünwald-Letnikov (G-L) fractional differential to improve contrast in brain tumour magnetic resonance imaging (MRI) scans. In this approach, the authors considered the correlation among pixel values to construct masks of specified sizes (3×3 and 5×5). The enhanced image is obtained by applying a framed mask to the input image, where the mask is selected based on individual pixel values in those three regions. Subsequently, the technique continues to evolve and adapt to achieve optimal image enhancement by using a gradient-based threshold.

Alternative techniques are employed in the frequency domain, where the image is transformed from the spatial domain. This transformation is achieved through wavelet transform methods, such as the discrete wavelet transform (DWT) (Kahlessenane et al., 2021), discrete cosine transform (DCT) (Fu et al., 2015). The primary objective of these methods is to improve the contrast and quality of an image while maintaining edge information. In Kallel & Ben Hamida (2017), singular value decomposition (SVD) method is exclusively applied to the low-frequency components of the input image generated using DWT, in order to maintain edges and mitigate potential deficiencies. An enhanced image is generated using an adaptive dynamic gamma correction function along with inverse SVD. This method was applied to improve image quality by maintaining the enhancement of specific frequency ranges and preserving edge information.

Recently, some deep learning-based methods (Liu & Tian, 2020) have been introduced for image enhancement. Image enhancement challenges were addressed by Panetta et al. (2023) by developing the Deep Perceptual Image Enhancement Network (DPIENet), an end-to-end trainable deep convolutional neural network. Their work utilizes the exposure variation in order to restore an image from a single image by synthesizing multiple exposures from the same image. Deep learning-based image enhancement methods can address issues (such as texture distortions, high-level noise, etc.) by acquiring compact feature representations and performing nonlinear up sampling to reconstruct enhanced images.

However, the performance of deep learning models typically depends on the availability of sufficiently large and diverse training datasets to ensure better accuracy and generalization. In limited-data scenarios, training such models can become computationally intensive and may lead to overfitting, particularly in medical imaging. Moreover, over-enhancement in some cases may amplify noise or alter minor structural details. Image quality deterioration can significantly affect both human interpretation and the performance of computer-assisted methods in medical imaging. Therefore, the implementation of image enhancement techniques is crucial for accurately interpreting medical images and facilitating effective computer-based analyses.

The rest of the paper is divided into varied sections: Section 2 comprises related work. Section 3 discusses the fundamental principles of the study. Section 4 highlights the methodology and its implementation.

Results and discussion are presented in Section 5, followed by the paper's conclusion and future applications in Section 6. The detailed abbreviations list used in this paper is provided in **Table 1**.

Table 1. Abbreviations repository.

Abbreviations	Descriptions
AMBE	Absolute mean brightness error
BBHE	Brightness preserving bi histogram equalization
BHEMHB	Bi-histogram equalization using modified histogram bins
BHEPL	Bi-histogram equalization with a plateau limit
CLAHE	Contrast limited adaptive histogram equalization
DPIENet	Deep perceptual image enhancement network
DWT	Discrete wavelet transform
GMSD	Gradient magnitude similarity deviation
GMS	Gradient magnitude similarity
HE	Histogram equalization
IDWT	Inverse discrete wavelet transform
IEHE	Intensity exposure histogram equalization
LIME	Low-light image enhancement
MOS	Mean opinion score
PCA	Principal component analysis
PSNR	Peak-signal-to-noise ratio
PSO	Particle swarm optimization
REC	Relative enhancement in contrast
RSHE	Recursive sub-histogram equalization
SFDWT	Spatial frequency discrete wavelet transform
SF	Spatial frequency
SSIM	Structural similarity index
SVD	Singular value decomposition
SV	Singular value matrix
TCDHE	Triple clipped dynamic histogram equalization

2. Related Work

Various algorithms have been proposed in the literature to improve the quality and contrast of different types of images. A popular contrast enhancement technique is the HE algorithm. Its principle is based on distributing intensity values over a given image's dynamic range based on its cumulative histogram, but HE sometimes induces unwanted artifacts such as over-enhancement and intensity saturation. To overcome these artifacts, Kim (1997) proposed a novel extension of histogram equalization called the BBHE. In BBHE, an input image is decomposed into two sub-images based on its mean brightness, and after certain operations, the sub-images are combined to produce the output image.

Ooi et al. (2009) proposed Bi-histogram equalization with a plateau limit (BHEPL) method for image enhancement. The method was designed to maintain the image's mean brightness by decomposing its original histogram into two sub-histograms. To avoid over-enhancement in images, the authors clipped these sub-histograms using the calculated plateau value. Tang & Mat Isa (2017) introduced a novel methodology Bi-histogram equalization using modified histogram bins (BHEMHB), by incorporating the features of bi-histogram equalisation. The method was designed to improve the overall information content by preserving the image's mean brightness, thereby reducing the limitations observed in HE. In BHEMHB, the input image histogram is divided at the median intensity value, and the resulting histogram bins are then combined to produce the output image.

Joseph & Periyasamy (2018) proposed a method based on HE for enhancing medical images, specifically MRI. As observed in HE, it tends to over-enhance certain grey levels, producing increased saturation and amplified noise. The authors developed this method to address such issues by clipping the histogram height

at the most frequent grey levels to avoid noise amplification while also preserving natural image features. The study lacks a method for determining the optimal threshold, which is considered a shortcoming.

Singh & Bhandari (2021) proposed a novel Low-light image enhancement (LIME) algorithm using the reflection model and PCA. The algorithm works adaptively for dark images, correcting colour distortion and converting RGB colour images to HSV colour space. Principal component analysis (PCA) based on image fusion is designed to capture relevant features from the images. Then, the contrast-limited adaptive histogram equalization (CLAHE) model is applied to improve global contrast.

A recursive sub-histogram equalization (RSHE) method based on linear regression was implemented by Chaudhary et al. (2022) to enhance the contrast of an image. In this method, the image's histogram is divided into two disjoint sub-histograms, each computed by averaging all intensity values. In each segmented partition, intervals are created based on the regression line and histogram, which are fitted to each set of points in the corresponding sub-histograms using the least squares method. HE-based methods (Wang et al., 1999; Zuo et al., 2013) preserve the smooth regions of an image, so as to enhance the sharp features, like high frequency or detailed components (edges, textures, etc.) within an image, in the frequency domain (Sugamya et al., 2016) methods have been developed and presented in the literature.

Demirel et al. (2010) implemented a new satellite image contrast enhancement technique using DWT and SVD. Atta & Abdel-Kader (2015) proposed a modified version of enhancement techniques for low contrast images based on SVD, for preserving the mean brightness of an image. Some low-contrast images are not satisfactorily enhanced by this technique because it scales the singular value matrix. This method calculates the weighted sum of the singular value matrices corresponding to the original image and the enhanced image generated using HE to obtain the modified singular values for the equalized image.

Sandeepa et al. (2017) proposed a method that combines spatial and frequency-domain techniques to decompose the input image. A mask is formulated by subtracting the inverse SVD from the reconstructed approximation coefficient matrix to obtain a contrast residual. The resulting mask is then merged with the IEHE image to improve contrast.

Sahnoun et al. (2019) presented a modified approach using the DWT-SVD technique to enhance low-contrast T1-w brain MR Images for brain tissue exploration. This method uses the DWT technique on the equalized image using the HE algorithm. Then SVD is applied on the decomposed LL sub band, to generate the singular value matrix and compute the modified approximated coefficients. A new singular value matrix is generated using the aggregated sum of the singular values from the original and equalized images, respectively. Hence, the enhanced image is reconstructed using inverse SVD and inverse DWT processes. Jinju et al. (2019) proposed a multi-resolution image fusion technique based on SFDWT technique for applications to remote sensing images. The method involved resampling of a low-resolution MS (multispectral image) image to a high-resolution PAN (panchromatic image) image. For this resampling, the spectral and spatial information from both images was fused from their corresponding wavelet coefficients. The authors, Saifullah & Dreżewski (2023) have applied hybrid methods that integrate HE and CLAHE features to improve CNN-based segmentation performance in chest X-ray and CT imaging tasks. Similarly, the subsequent method developed by Ahmad et al. (2025) demonstrated that contrast enhancement methods positively influence deep learning frameworks such as U-Net and Mask R-CNN by improving boundary clarity and structural visibility in medical images. However, these techniques primarily focus on improving downstream segmentation accuracy rather than on preserving structural features and enhancing multi-scale information during the improvement stage itself.

Furthermore, fuzzy-based hybrid methods combined with CLAHE have been implemented for retinal image enhancement to improve local contrast and vessel visibility (Shaout & Han, 2023). While adaptive, such spatial-domain approaches may introduce additional complexity and the risk of over-enhancement in consistent regions of the images. In contrast, the proposed method is designed using hybrid HE, a 2-level DWT with SVD and spatial frequency-based fusion, enabling controlled enhancement while preserving structural integrity. By integrating spatial and frequency-domain processing, the proposed method addresses limitations of spatial-domain techniques and provides an enhancement method for medical imaging applications.

The aim of this paper is to propose a simple framework for improving contrast and feature enhancement in medical images, with a specific focus on MRI, ultrasound, and X-ray images. This method combines the features of both the enhanced and input images. In the proposed method, an equalised histogram of the input image is obtained using the TCDHE technique (Kumar et al., 2021). Furthermore, a 2-level DWT and SVD method is applied to both images separately to enhance their subbands, considering the detailed and approximated components within each image. Preserving the high-frequency content is of vital importance for accurate localization and to preserve edge information in the image (Joseph & Periyasamy, 2018), due to which the SF method is applied on the high-frequency components generated using the DWT decomposition. Eventually, the enhanced image is reconstructed using the IDWT, resulting in better contrast and preserved edge details.

2.1 Motivation and Contribution

Computer-aided diagnosis is advancing, accelerating improvements and developments in medical imaging. Medical image analysis is essential for evaluating and optimizing treatment strategies to improve patient health. However, due to insufficient illumination, it becomes difficult to monitor and analyse medical scans, resulting in poor contrast medical images. Many research studies have introduced innovative techniques for image contrast enhancement to address real-world problems.

Image enhancement procedures can improve the visualization of tissues identified as anomalies. These enhanced images can help precisely identify the disorder associated with specific medical conditions. The motivation for this research is to design, formulate, and implement a hybrid image enhancement method that combines HE, DWT, and spatial-frequency techniques.

In the preceding publications (Demirel et al., 2010; Kumar et al., 2021), a deficiency was observed in the lack of a detailed subjective assessment parameter that effectively demonstrates the algorithm's efficiency in visual evaluation, such as MOS. Also, the previous work limited the method's applicability to two datasets comprising only two modalities. The proposed method aims to address the limitations of conventional HE-based techniques and some recent methods discussed above. This paper proposes a hybrid method that combines elements from existing and state-of-the-art techniques. The evaluation metrics used for quantitative assessment revealed improved outcomes in certain cases, while securing second-best results in others. We have demonstrated that all the performance metrics considered deliver better results than alternative methodologies. This research aims to advance medical image enhancement by offering improved solutions. Some of the contributions are highlighted below:

- The proposed method is implemented on three distinct medical datasets (MRI, X-ray and ultrasound) to demonstrate the efficacy and versatility of the application.
- The proposed method finds a modified improvement factor (η) using Equation (21) which is used to evaluate the improved SV ($\Sigma_{(LL)_m}$) given by Equation (22). The improved singular value matrix value is then used to compute the enhanced LL_{new} sub-band using ISVD.

- The proposed method integrates spatial frequencies of the enhanced image derived by TCDHE with the transformed image obtained through DWT to effectively retain the detailed components of the image, including edges and sharp features.
- The average values for all performance metrics, along with their corresponding standard deviations, have been calculated for each of the three categories of medical images.
- The paper includes a subjective assessment of the enhanced output images, supported by their mean opinion score collected from several medical experts.

3. Fundamental Principles

This section briefly discusses about the preliminaries associated with the DWT, SVD and SF.

3.1 SVD

The singular value decomposition is the process of factorization of a matrix A into the product of three matrices, $A = UDV^T$ where U and V have orthonormal columns and D is a diagonal matrix with positive real entries. This computation allows retaining the important singular values that contribute to image quality while discarding the unwanted (non-essential) values. The singular values of an $m \times n$ matrix A are defined as the square roots of the eigenvalues computed from the $m \times m$ matrix AA^T.

The SVD process has various applications, including watermarking images, computing weighted least-squares estimates, image enhancement, and optimal prediction.

3.2 DWT

In DWT, an image is analysed using a filter bank of low- and high-pass filters at each decomposition level. High-pass filters (H) capture the finer details to be extracted from an image (such as edges and textures), whereas low-pass filters (L) focuses on the approximate information within the image (Kahlessenane et al., 2021). The DWT process separates the low and high frequency components of an image into four sub bands, which are obtained using Equations (1)-(4).

$$LL(u,v) = \frac{g(u,v)+g(u,v+1)+g(u+1,v)+g(u+1,v+1)}{2} \quad (1)$$

$$LH(u,v) = \frac{g(u,v)+g(u,v+1)-g(u+1,v)-g(u+1,v+1)}{2} \quad (2)$$

$$HL(u,v) = \frac{g(u,v)-g(u,v+1)+g(u+1,v)-g(u+1,v+1)}{2} \quad (3)$$

$$HH(u,v) = \frac{g(u,v)-g(u,v+1)-g(u+1,v)+g(u+1,v+1)}{2} \quad (4)$$

The 2-level DWT transform consists of 1D transformations applied along the vertical and horizontal components i.e. along the image's rows and columns. The transformation then decomposes the image into four sub-bands that are LL: low-frequency components; LH: low-frequency (taken along the horizontal) and the high-frequency components (in the vertical direction); HL: high and low frequency components; and HH: high-frequency components. These sub-band images encompass the frequency components of the original image. This layered organization of the transformed image enables the identification of both small and large features present in an image, as represented in **Figure 1**. The coefficients of each sub-band can be derived by employing the Haar filter.

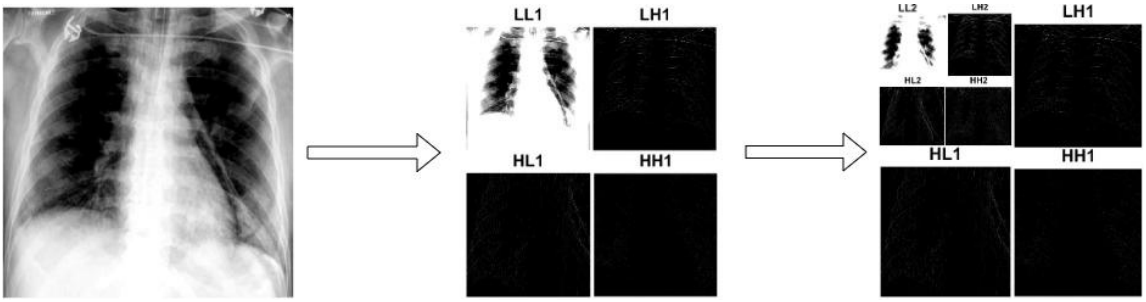

(a) (b) (c)

Figure 1. DWT process for (a) Input image, (b) 1-level DWT and (c) 2-level DWT.

3.3 Spatial Frequency

SF quantifies the amount of high-frequency content in an image, reflecting its sharpness and clarity. The higher SF value provides greater clarity in the image. In medical image enhancement, preserving the detailed features of an image, such as edges and boundaries, is crucial for the precise detection of medical anomalies. The SF of an image can be computed using the equation below, where r_f and c_f represent the row and column frequencies of the image.

$$sf = \sqrt{{r_f}^2 + {c_f}^2} \tag{5}$$

$$r_f = \sqrt{\frac{1}{MN} \sum_{p=0}^{M-1} \sum_{q=1}^{N-1} \big(I(p,q) - I(p,q-1)\big)^2} \tag{6}$$

$$c_f = \sqrt{\frac{1}{MN} \sum_{q=0}^{N-1} \sum_{p=1}^{M-1} \big(I(p,q) - I(p-1,q)\big)^2} \tag{7}$$

4. Proposed Methodology

The proposed methodology is thoroughly explained in this section. The TCDHE approach is first applied to the input image, followed by a 2-level DWT applied to both the input and the TCDHE-enhanced image. Then SVD is used to transform the LL bands and obtain the modified approximated coefficients. The SF method is used to find modified detailed coefficients. Next, IDWT is used to combine all the modified coefficient matrices to get an enhanced image. The detailed process is depicted in **Figure 2**.

Consider an input image (I) of size 512×512, and create the histogram f_k corresponding to each pixel in the image, where $k \in (0, 255)$. Then the histogram is divided into three sections using the intensity values r_1 and r_2 computed through Equations (8) and (9).

$$r_1 = \mu - 0.43\,\sigma \tag{8}$$

$$r_2 = \mu + 0.43\,\sigma \tag{9}$$

where, μ and σ are the average intensity value and standard deviation of the input image (I). To restrict the slope of the mapping function at the most frequent grey levels, one can decrease the histogram's height at those levels. This can be accomplished by simply clipping the histogram based on a predetermined threshold. The threshold serves as a reference point to determine which grey levels should be clipped by the clipping operation. The threshold values (τ_j) by which the histogram in each sub-section needs to be clipped has been computed using the Equation (10).

$$\tau_j = \frac{1}{I_m} \sum_{k=I_o}^{I_m} f_j(k) \; ; j = 1, 2, 3 \tag{10}$$

here, I_m and I_o are the maximum and minimum intensity values within each sub-region and $f_j(k)$ is the corresponding histogram of each sub-region $(j = 1, 2, 3)$. After clipping, the resulting histogram is evaluated as

$$f_c(k) = \begin{cases} f_j(k), & f_j(k) < \tau_j \\ \tau_j, & f_j(k) \geq \tau_j \end{cases} ; \; j = 1, 2, 3 \; , k = 0, \dots, 255 \tag{11}$$

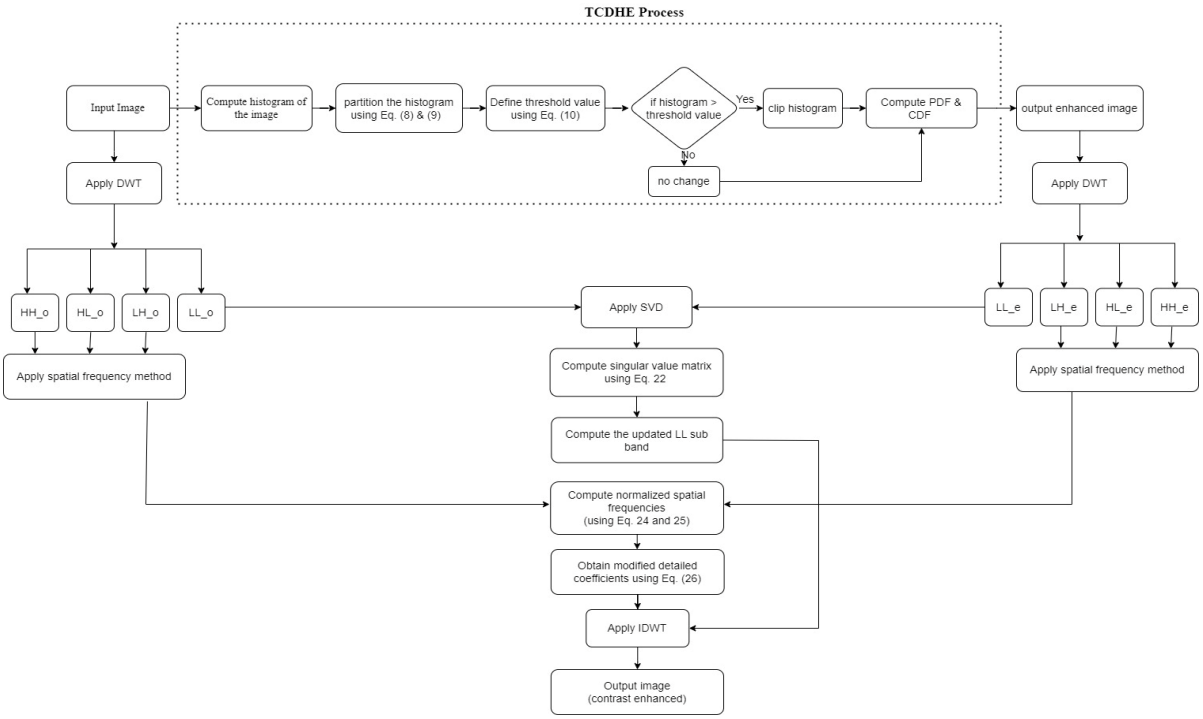

Figure 2. The block diagram of the proposed method.

After the redistribution of the pixels, Equations (12) and (13) can be employed to compute the PDF and CDF of each clipped histogram $f_c(k)$.

$$pdf(k) = \frac{f_c(k)}{n_j} \tag{12}$$

$$cdf(k) = \sum_{k=I_o}^{I_m} pdf(k) \tag{13}$$

where, n_j is the total number of pixels in each clipped histogram. Subsequently, each subregion then undergoes a mapping procedure that transforms its dynamic range to balance the equalization process. This can be achieved using the Equations (14)-(17).

$$s_o = 0 \tag{14}$$

$$s_1 = \frac{r_1 - r_0}{r_3 - r_0 + 1} \; (L - 1) \tag{15}$$

$$s_2 = \frac{r_2 - r_1}{r_3 - r_0 + 1}(L-1) + s_1 \quad (16)$$

$$s_3 = L - 1 \quad (17)$$

where, r_o and r_3 represent the lowest and highest grey level value in the image, respectively, and L denote the maximum intensity values in the image. After the acquisition of the new dynamic ranges (s_o, s_1, s_2, s_3), each sub-region is remapped using the Equations (18)- (20) to obtain the enhanced pixel values.

$$t_l = (s_1 - 1)\, cdf_l(k) \quad (18)$$

$$t_m = s_1 + (s_2 - 1 - s_1)\, cdf_m(k) \quad (19)$$

$$t_u = s_2 + (s_3 - s_2)\, cdf_u(k) \quad (20)$$

where, $cdf_l(k)$, $cdf_m(k)$ and $cdf_u(k)$ are the lower, middle, and upper cumulative probabilities calculated corresponding to each sub-region. The enhanced image (I_e) is obtained by the amalgamation of t_l, t_m, and t_u.

The enhanced image obtained through TCDHE serves as input to the next level, where it undergoes a 2-level DWT. Additionally, the original input image is simultaneously subjected to DWT. Using the DWT, the image is decomposed into sub-bands, each consisting of detailed and approximated image coefficients. The approximated coefficients consist of the LL_o and LL_e, which are derived from the original input image and the TCDHE-enhanced image, respectively. After that, the approximated coefficients undergo the application of SVD, resulting in the acquisition of decomposed matrices V_{LL_o}, U_{LL_o}, Σ_{LL_o}, as well as V_{LL_e}, U_{LL_e}, Σ_{LL_e}, correspondingly. Following this, the improvement factor (η) is computed using the Equation (21), considering the minimum values obtained from V_{LL_o}, U_{LL_o} and V_{LL_e}, U_{LL_e}. This improvement factor is subsequently employed to derive the modified singular value matrix $\left(\Sigma_{(LL)_m}\right)$ and the enhanced low-frequency components, denoted as LL_{new}, using the Equations (22) and (23), respectively.

$$\eta = \frac{(1 - \min(U_{LL_e})) + \min(V_{LL_e})}{(1 - \min(U_{LL_o})) + \min(V_{LL_o})} \quad (21)$$

$$\Sigma_{(LL)_m} = \theta\eta\Sigma_{LL_e} + \frac{(1-\theta)}{\eta}\Sigma_{LL_o} \quad (22)$$

$$LL_{new} = U_{LL_o}\, \Sigma_{(LL)_m}\, {V_{LL_o}}^T \quad (23)$$

Based on empirical investigation, the value of theta is set to 0.2. Once the updated approximated coefficient band is obtained, spatial frequencies of the detailed coefficients from both the input image (LH_o, HL_o, HH_o) and the TCDHE-enhanced image (LH_e, HL_e, HH_e) are calculated using the Equations (5)-(7). Then, these spatial frequencies associated with each sub-band undergo normalization using Equations (24)-(25). Finally, these normalized spatial frequencies are fused together according to the Equations (26) to achieve enhanced higher frequency sub-bands.

$${sf_{LH_o}}^N = \frac{sf_{LH_o}}{sf_{LH_o} + sf_{LH_e}} \quad (24)$$

$${sf_{LH_e}}^N = \frac{sf_{LH_e}}{sf_{LH_o} + sf_{LH_e}} \quad (25)$$

$$LH_{new} = {sf_{LH_o}}^N LH_e + {sf_{LH_e}}^N LH_o \quad (26)$$

In a similar manner, other detailed sub-bands (HL_{new}, HH_{new}) are modified by using the normalised detailed coefficients corresponding to the respective bands. Finally, IDWT is applied to all the updated sub-bands $(LL_{new}, LH_{new}, HL_{new}, HH_{new})$ resulting in the reconstruction of the improved output image (I_o).

TCDHE effectively enhances contrast, DWT enables multi-resolution analysis and separation of frequency components, and SVD helps maintain crucial structural and illumination features.

***Algorithm steps*:**
Step 1: *Read the input image* (I) *of* 512×512 *dimension.*
Step 2: *Apply TCDHE to obtain an enhanced image,* (I_e) [*using Equations* (8)-(20)].
Step 3: *Apply DWT decomposition*
$DWT\ (I) \rightarrow LL_o, LH_o, HL_o, HH_o$ *sub bands*
$DWT\ (I_e) \rightarrow LL_e, LH_e, HL_e, HH_e$ *sub bands*
Step 4: *Apply SVD on both the images* (I) *and* (I_e) *approximated sub bands,* LL_o *and* LL_e.
$SVD\ (LL_o) \rightarrow V_{LL_o}, U_{LL_o}, \Sigma_{LL_o}$
$SVD\ (LL_e) \rightarrow V_{LL_e}, U_{LL_e}, \Sigma_{LL_e}$
Step 5: $\eta \leftarrow$ *compute using Equation* (21) *// Compute improvement factor*.
Step 6: *Updated singular value matrix* $\Sigma_{(LL)_m}$ *is then obtained using Equation* (22).
Step 7: *Singular value matrix* $\Sigma_{(LL)_m}$ *in above step is used to compute the updated approximated* LL_{new} *sub band.*
Step 8: *After step 8, the spatial frequencies* (*sf*) *of each detailed sub-band are calculated using Equations* (24)-(26).
Step 9: *Inverse DWT is applied to reconstruct the image.*
$IDWT\ LL_{new}, LH_{new}, HL_{new}, HH_{new} \rightarrow I_o$
Step 10: *Final output image* (I_o) *generated is contrast-enhanced.*

5. Results and Discussions

This section discusses the performance of the proposed method through quantitative and qualitative analysis. To evaluate the performance of the proposed method relative to other techniques, all results are computed using state-of-the-art methods on the same dataset. Also, to provide a detailed assessment of the proposed method's efficiency, the comparison techniques have been carefully selected, including a wide range of approaches for enhancing image contrast. For the numerical evaluation of the proposed method, six performance metrics, such as AMBE, PSNR, SSIM, REC, entropy, and GMSD, have been considered. The results obtained for these parameters are compared with other existing techniques, like DWT_SVD (Demirel et al., 2010), MT_PSO (Wadhwa & Bhardwaj, 2021), TCDHE_SF (Kumar et al., 2021), and also with some standard methods such as HE, CLAHE, and BBHE.

The experimental evaluation is conducted using the dataset (https://github.com/ieee8023/covid-chestxray-dataset, Gandhamal et al., 2017), including X-ray, ultrasound, and MRI images (https://www.kaggle.com/datasets/navoneel/brain-mri-images-for-brain-tumor-detection). The dataset consists of 300 X-ray images with a resolution of 1935×2400 pixels in TIFF format, 322 ultrasound images with a resolution of 390×330 pixels, and 253 MRI greyscale medical images. For quantitative evaluation, a total of 150 images from the original dataset are processed using the proposed methodology and comparative methods. The final datasets comprise 50 images from each modality: brain MRI, chest X-ray, and ultrasound. The experiments are conducted in MATLAB (R2022a) software on a system equipped with an Apple M2 processor and 8 GB RAM. The average processing time per 512×512 image is approximately in the range $(0.3 - 1.5)$ seconds, including all three modalities. For the purpose of

compactness, the results include values of performance metrics, including AMBE, REC, PSNR, GMSD, SSIM, and entropy, measured for 15 test images (**Table 3**), and the results of six images are considered for the comparison and visualization assessment. The parameter θ is selected through empirical experimentation to balance enhancement strength and artifact suppression. Preliminary trials indicated that values in the range of $0.1 - 0.5$ produced comparable visual and quantitative performance, with $\theta = 0.2$ yielding the best result for contrast enhancement and preservation of structural details. A brief sensitivity analysis is presented in **Table 2** for different values of this parameter; the method demonstrated stable behaviour over this range.

The analysis of the data obtained reveals that the proposed method exhibits lower AMBE and GMSD values, higher SSIM and PSNR values, and satisfactory REC and entropy values. The data validates the claim that the proposed method significantly improves the quality and contrast of an image.

Table 2. Average of evaluation metrics computed for 10 medical (including MRI, X-ray and ultrasound) images for different values of θ.

θ	Evaluation parameters						
	AMBE	**GMSD**	**PSNR**	**SSIM**	**Original entropy**	**Enhanced entropy**	**REC**
0	8.9628	0.1590	31.42	0.98	6.4582	6.4667	0.9864
0.1	7.4314	0.1555	32.61	0.98	6.4582	6.4851	0.9841
0.2	5.8866	0.1531	34.65	0.99	6.4582	6.4949	0.9819
0.3	4.6330	0.1544	35.33	0.99	6.4582	6.5007	0.9802
0.4	3.6640	0.1590	37.22	0.99	6.4582	6.5130	0.9788
0.5	3.4985	0.1595	35.65	0.99	6.4582	6.5229	0.9777

5.1 Quantitative Assessment

In this section, a brief description of the performance metrics chosen for the objective evaluation of the proposed method is provided. The chosen parameters aim to assess the effectiveness of the proposed method by quantifying various aspects of the input and output images, including quality, structural features, edge information, noise content, and other relevant characteristics.

Table 3. Performance metrics evaluated using proposed method.

Images	AMBE	GMSD	PSNR	SSIM	Original Entropy	Enhanced Entropy	REC
X_1	0.6922	0.0631	49.7040	0.9998	7.5181	7.5110	1.0015
X_2	1.4771	0.0857	43.9590	0.9996	7.1739	7.1598	1.0021
X_3	8.4246	0.1618	29.4100	0.9973	7.2169	7.1370	1.0093
X_4	1.7794	0.1173	41.9210	0.9992	7.6266	7.6358	0.9969
X_5	0.3343	0.0952	52.8680	0.9996	7.5850	7.5714	1.0015
M_1	1.8711	0.0702	38.2750	0.9990	5.9132	5.9432	0.9897
M_2	0.6525	0.0753	46.4470	0.9996	4.2938	4.2717	1.0051
M_3	0.0239	0.0678	59.4850	0.9998	6.2165	6.2131	0.9994
M_4	0.1576	0.1308	49.5300	0.9988	5.7221	5.7480	0.9974
M_5	0.6089	0.0451	48.5980	0.9998	5.0791	5.0714	1.0038
U_1	2.5520	0.1546	35.0860	0.9937	6.1609	6.2703	0.9741
U_2	0.3479	0.0925	48.0420	0.9990	3.7210	3.7431	0.9822
U_3	0.1420	0.1074	53.1180	0.9989	6.0695	6.0687	0.9964
U_4	0.1161	0.0983	52.8820	0.9992	4.9978	4.9955	0.9962
U_5	3.2966	0.2096	27.1320	0.9715	3.7610	3.4728	0.8969

AMBE: This metric (Rao, 2020) quantifies the disparity in average brightness between the input and output image and is calculated using Equation (27) as

$$AMBE = |\mu_o - \mu_e| \tag{27}$$

where, μ_o and μ_e are the average intensity values of the input image and output images. A lower AMBE value indicates better preservation of image brightness. **Table 3** reveals that the AMBE values for 15 sample images are exceptionally low, which demonstrates the efficiency of the proposed method in preserving the natural brightness of the input image.

Table 4. Comparative analysis of methods based on AMBE values.

Images	Proposed	DWT_SVD	HE	TCDHE_SF	BBHE	CLAHE	MT_PSO
X_1	0.6922	18.0870	26.0190	5.6527	0.9504	0.5062	32.3826
X_2	1.4771	32.3160	37.3050	16.1430	7.3227	26.7450	20.2203
X_3	8.4246	29.3450	39.7900	6.2187	13.0480	18.3430	21.575
X_4	1.7794	17.6190	23.9360	8.8100	3.7298	1.7603	16.0664
M_1	1.8711	42.9020	79.0160	5.9664	30.3760	17.2790	11.0015
U_1	2.5520	59.9270	104.0200	5.9878	24.7670	36.3990	16.5281

The analysis of the data presented in **Table 4** validates that the proposed method effectively preserves the brightness of the output image. This conclusion is supported by the lower AMBE values obtained with the other methods under consideration. These findings confirm that the proposed method outperforms existing and state-of-the-art techniques in terms of efficiency.

PSNR: It is a measure used to assess the difference in quality between the input and output images by quantifying the reduction in noise level (Aosiman et al., 2020). Image quality is higher when PSNR is higher, indicating lower distortion.

$$PSNR = 10\log_{10}\left[\frac{255^2}{\sum_u\sum_v|O(u,v)-E(u,v)|^2}\right] \tag{28}$$

where, O is the original image and E is the output image, $u = 1, \dots, m$ and $v = 1, \dots, n$. The legends from top to bottom in **Figure 3** correspond to the columns of an image from left to right, respectively, in a grey-scale print. From **Figure 3**, it is evident that the proposed scheme maintains the quality of the original image while simultaneously reducing noise, surpassing existing techniques and certain benchmark methods. Comparatively, the lower PSNR value is associated with HE, as this method induces over enhancement; DWT_SVD also shows the lowest PSNR, indicating higher noise levels and reduced image clarity. MT_PSO, CLAHE, and BBHE have low values for this metric, and BBHE and MT_PSO have poor values for the MRI and ultrasound datasets. Notably, the PSNR value for TCDHE_SF is deemed satisfactory for all the datasets considered. The proposed method achieves the highest PSNR, demonstrating its efficiency.

SSIM: An evaluation of the similarities between an output image and its original is performed using this metric (Gandhamal et al., 2017) and computed using Equation (29) as

$$SSIM = \frac{(2\,\mu_O\,\mu_E + c_1)(2\,\sigma_{OE} + c_2)}{(\mu_O{}^2 + \mu_E{}^2 + c_1)\,(\sigma_O{}^2 + \sigma_E{}^2 + c_2)} \tag{29}$$

where, μ_O and μ_E are the mean intensity values of the original and enhanced images, and σ_{OE} represents the correlation between images O and E; ${\sigma_O}^2$ and ${\sigma_E}^2$ is the variance computed for each image O and E; c_1 and c_2 are the constants. The SSIM value ranges from 0 to 1, where values closer to 1 indicate less distortion and better feature preservation in the resultant image.

The SSIM values obtained using the suggested and state-of-the-art schemes are presented in **Table 5**. This table clearly visualizes that the proposed method achieves the highest SSIM value, indicating minimal degradation in the structural quality of the output image. It is further observed that the SSIM values for all the images taken from different modalities are very close to 1 as compared to the state-of-the-art methods.

The values of this metric also confirm that the proposed method effectively maintains the contrast and structural features of the enhanced image and demonstrates superior performance compared to HE, CLAHE, BBHE, and MT_PSO. Additionally, the results are satisfactory for methods like DWT_SVD and TCDHE_SF. Overall, the proposed method demonstrates superior performance by preserving the image's original features and achieving higher values.

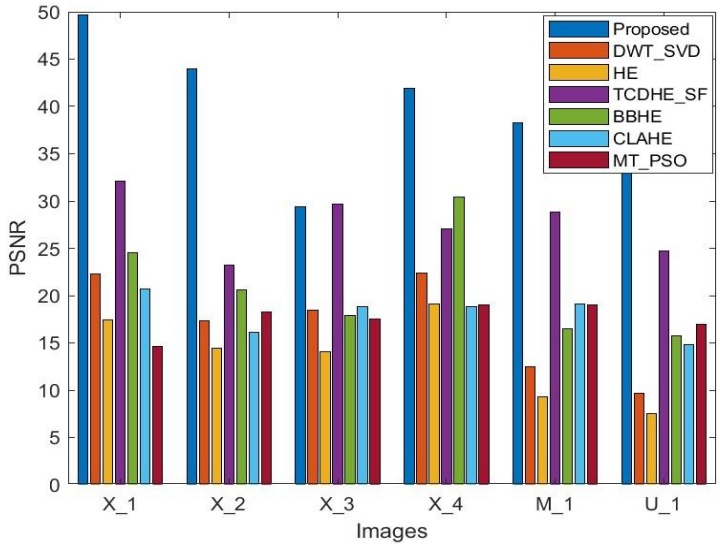

Figure 3. PSNR values computed for six medical images using different methods.

Table 5. Quantitative assessment of SSIM values among different enhancement techniques.

Images	Proposed	DWT_SVD	HE	TCDHE_SF	BBHE	CLAHE	MT_PSO
X_1	0.9998	0.9901	0.8651	0.9960	0.9334	0.8433	0.8702
X_2	0.9996	0.9703	0.7512	0.9760	0.8285	0.7418	0.8565
X_3	0.9973	0.9766	0.7859	0.9913	0.8666	0.7979	0.8760
X_4	0.9992	0.9900	0.8894	0.9947	0.9789	0.8436	0.8807
M_1	0.9990	0.6736	0.3688	0.9897	0.5495	0.6942	0.8752
U_1	0.9937	0.3673	0.2454	0.9632	0.7328	0.4853	0.7836

GMSD: The GMSD (Xue et al., 2014) measures the range of distortion severities in an image by computing pixel-wise GMS and the standard deviation of GMS, as given by Equations (30)-(32). $GMS(l) \in [0,1]$, with 1 indicating perfect structural similarity at the pixel level l.

$$GMS(l) = \frac{2\, gm_h(l)\, gm_v(l)+c}{gm_h{}^2(l)+gm_v{}^2(l)+c} \tag{30}$$

where, l denotes the location along vertical (v) and horizontal (h) gradient images and their magnitudes are gm_v and gm_h, respectively.

$$GMSM = \frac{1}{N} \sum_{l=1}^{N} GMS(l) \tag{31}$$

and,

$$GMSD = \sqrt{\frac{1}{N} \sum_{l=1}^{N} (GMS(l) - GMSM)^2} \tag{32}$$

As shown in **Figure 4**, the GMSD value is highest for images obtained with MT_PSO, as it fails to preserve image gradients, leading to greater distortion and lower image quality. The HE-generated image is the next higher value for this metric because it loses the image's fine details. In the CLAHE and BBHE methods, the GMSD value is also considerably higher due to over-enhancement. The images generated using DWT_SVD and TCDHE_SF show satisfactory results, but the proposed method has the lowest value for this performance metric, supporting the claim that it preserves image gradients and overall quality. In the present study, the observed GMSD values ranged from $(0.05 - 0.45)$ using the proposed method, which consistently achieves lower distortion than other methods. For medical images, the values typically fall within a short range (often approaching 0 depending on the dataset).

Entropy: This metric (Chandra & Bhardwaj, 2024) calculates the average information of an image. The values closer to 1 represent that the output image has retained maximum information and is given as:

$$E = -\sum_k p(k)\log_2\big(p(k)\big) \tag{33}$$

where, $p(k)$ is the probability corresponding to the pixel values defined as $p(k) = n(k)/N$, $k \in [0, 255]$ and N: sum of intensity values. This parameter indicates the improvement in image detail compared to the original images. According to **Table 6**, the entropy value is highest in the images obtained with CLAHE, which can be attributed to the over-brightness introduced by CLAHE. Conversely, HE produces a lower entropy value, suggesting a compromise in the features and information content of the enhanced image. Other methods, such as BBHE, MT_PSO, and DWT_SVD, have entropy values closer to the original entropy but still lower than TCDHE_SF. In terms of this metric, the proposed method demonstrates satisfactory results compared to other methods, except for CLAHE.

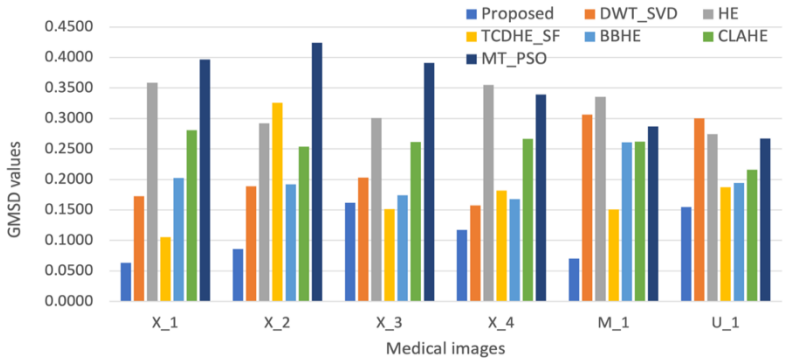

Figure 4. GMSD values computed for six medical images using different methods.

Table 6. Evaluation of enhancement techniques using entropy.

Images	Original	Proposed	DWT_SVD	HE	TCDHE_SF	BBHE	CLAHE	MT_PSO
X_1	7.5181	7.5110	7.3393	5.9678	7.5410	7.2214	7.5828	6.3116
X_2	7.1739	7.1598	6.8804	5.7938	6.6505	7.0167	7.6843	5.6965
X_3	7.2169	7.1370	6.9350	5.9410	7.3407	7.1402	7.6662	6.4521
X_4	7.6266	7.6358	7.4505	5.9527	7.5339	7.4902	7.7545	7.3917
M_1	5.9132	5.9432	5.8285	4.7461	5.6936	5.5730	6.9874	5.9586
U_1	6.1609	6.2703	6.6466	4.6088	6.1528	5.9182	7.2073	6.4779

REC: It (Joseph & Periyasamy, 2018) measures the enhancement in the contrast of an image by computing the difference in the brighter and darker regions in the image, and is given by Equation (34).

$$REC = \frac{C_O}{C_E} \tag{34}$$

where,

$$C_O = 20 \log 10 \left[\frac{1}{mn}\sum_{u=1}^{m}\sum_{v=1}^{n}\left(O(u,v)^2 - \left(\frac{1}{mn}\sum_{u=1}^{m}\sum_{v=1}^{n} O(u,v)\right)^2\right)\right] \tag{35}$$

and C_O *and* C_E are the contrast of the original and enhanced images. [C_E computed in a similar manner as given by Equation (35)].

This assessment parameter quantifies the change in contrast between the output and input images. **Table 7** presents the results for this metric obtained with different enhancement techniques. It is evident that methods such as HE, BBHE, and CLAHE yield the lowest value for this parameter, whereas the REC values for DWT_SVD and TCDHE_SF methods demonstrate satisfactory results for X-ray images but not for ultrasound images. The proposed method provides a REC value closer to 1, which shows better contrast enhancement than other methods, except for the MT_PSO method. As in MT_PSO, the REC value is higher due to increased brightness, resulting in excessive contrast enhancement in the output image.

Table 7. REC values obtained for medical images using various enhancement methods.

Images	Proposed	DWT_SVD	HE	TCDHE_SF	BBHE	CLAHE	MT_PSO
X_1	1.0015	1.0313	0.9546	0.9899	0.9614	0.9977	1.0575
X_2	1.0021	1.0548	0.9711	0.9786	0.9797	0.9735	1.0398
X_3	1.0093	1.0523	0.8857	0.9743	0.8883	0.9372	1.0726
X_4	0.9969	1.0300	0.9848	0.9788	0.9896	1.0156	1.0244
M_1	0.9897	0.8948	0.9387	1.0328	0.9459	0.9665	1.0606
U_1	0.9741	0.7959	0.8896	0.9221	0.8481	0.8686	1.1637

The proposed enhancement technique is evaluated and validated by comparing it with other advanced techniques, using performance metrics. The dataset, containing 150 medical images are used for the evaluation. **Table 8** depicts the average and standard deviation of the evaluation metrics computed for the proposed and other existing methods. The data in the table below clearly demonstrate that the values obtained with the proposed method outperform those from state-of-the-art techniques across most metrics, indicating its superior performance in enhancing medical images. The proposed method achieved lower AMBE (4.08), higher PSNR (37.67), and superior SSIM (0.99), which is closer to 1, compared to previous enhancement methods. Although the entropy value is highest for CLAHE (6.60) due to excessive contrast enhancement, the proposed method follows closely behind (5.98). By improving the contrast of medical images, the proposed method has the potential to assist doctors in providing accurate diagnoses and administering appropriate treatment.

The proposed enhancement method consists of multiple processing stages (TCDHE, 2-level DWT decomposition, SVD, and spatial frequency-based approach). The multi-stage architecture incurs higher computational time than simple HE-based techniques. The most intensive component is the SVD operation, which exhibits cubic complexity with respect to matrix dimensions. The results obtained using the proposed method, in terms of performance gains in contrast enhancement and structural preservation, justify the additional processing time. While the proposed method employs a two-level DWT, increasing the decomposition level beyond two may impose an additional computational burden, increase memory usage, and result in a loss of finer image details. Increasing the decomposition levels excessively can also increase the risk of over-enhancement or artifact amplification during image reconstruction, specifically for medical

images where fine details are diagnostically relevant. Therefore, a two-level decomposition was selected to balance between contrast enhancement and structural preservation.

Although this study proposes a hybrid framework, it still relies on a histogram-based enhancement mechanism. As a result, it is subject to certain limitations inherent in such techniques, particularly under challenging imaging conditions. While the proposed method seeks to reduce these effects, it cannot guarantee the complete elimination of such artifacts. Future research could investigate learning-based approaches to better address these limitations and focus on computational optimization strategies for real-time applications.

5.2 Subjective Assessment

The proposed method is applied to a total of 150 medical images, including X-ray images, ultrasounds and MRI scans. For brevity, only six images are presented to assess the visual appearance and quality of the enhanced images generated by the proposed method. **Figure 5** (A.1-A.6) illustrates the original images, including four X-rays, one MRI, and one ultrasound image, sourced from the medical dataset for visual assessment. The effectiveness of the proposed approach is evaluated based on a qualitative analysis of the enhanced images' visual appearance. A comparison is made between the proposed method and other techniques, including TCDHE_SF, DWT_SVD, HE, BBHE, MT_PSO, and CLAHE, and the results are shown in **Figures 5** and **6**. The results demonstrate that the proposed method produces enhanced medical images with improved visual appearance while preserving the original image features. Moreover, the proposed method effectively mitigates over-enhancement, which can lead to excessive brightness, as observed with the HE and CLAHE techniques.

In **Figure 5** (B.1-B.6), the enhanced images obtained using BBHE exhibit over-enhancement, with darker regions becoming excessively dark and brighter areas becoming excessively bright due to the separation of pixel values based on the mean value. **Figure 5** (C.1-C.6) presents the images enhanced using TCDHE_SF, showing significant enhancement in specific regions of the brain MRI but amplification of higher grey-level values in the X-ray images, resulting in a loss of image features, such as the low visibility of soft tissues like para-aortic and paraspinal lines. The DWT_SVD-enhanced images in **Figure 5** (D.1-D.6) exhibit a washed-out effect on the X-ray images and increased brightness in the MRI and ultrasound images, leading to a loss of structural features. **Figure 6** (E.1-E.6) showcases the images enhanced using HE, which suffer from drawbacks such as over-enhancement, increased noise levels, loss of detail, and overall inferior output image quality. The CLAHE-enhanced images in **Figure 6** (F.1-F.6) exhibit degraded image quality, increased overall brightness (as supported by AMBE values in **Table 4**), and fail to preserve edge information and structural similarity (as indicated by the lower SSIM value in **Table 5**). The images obtained using the MT_PSO method in **Figure 6** (G.1-G.6) exhibit increased contrast and brightness but a loss of sensitivity (e.g., reduced visibility of the right atrium and the right paratracheal stripe), and they also induce blurriness in the X-ray images. In contrast, as observed in **Figure 6** (H.1-H.6), the proposed method retains structural similarity, preserves brightness-sensitive features, and maintains overall image quality, resulting in contrast-enhanced images. The enhanced images obtained using the proposed method reduce image noise and provide better results on the given medical dataset than other existing and benchmark methods. The output images are suitable for further processing and can be easily interpreted by medical professionals, enabling them to provide accurate diagnoses and effective treatments.

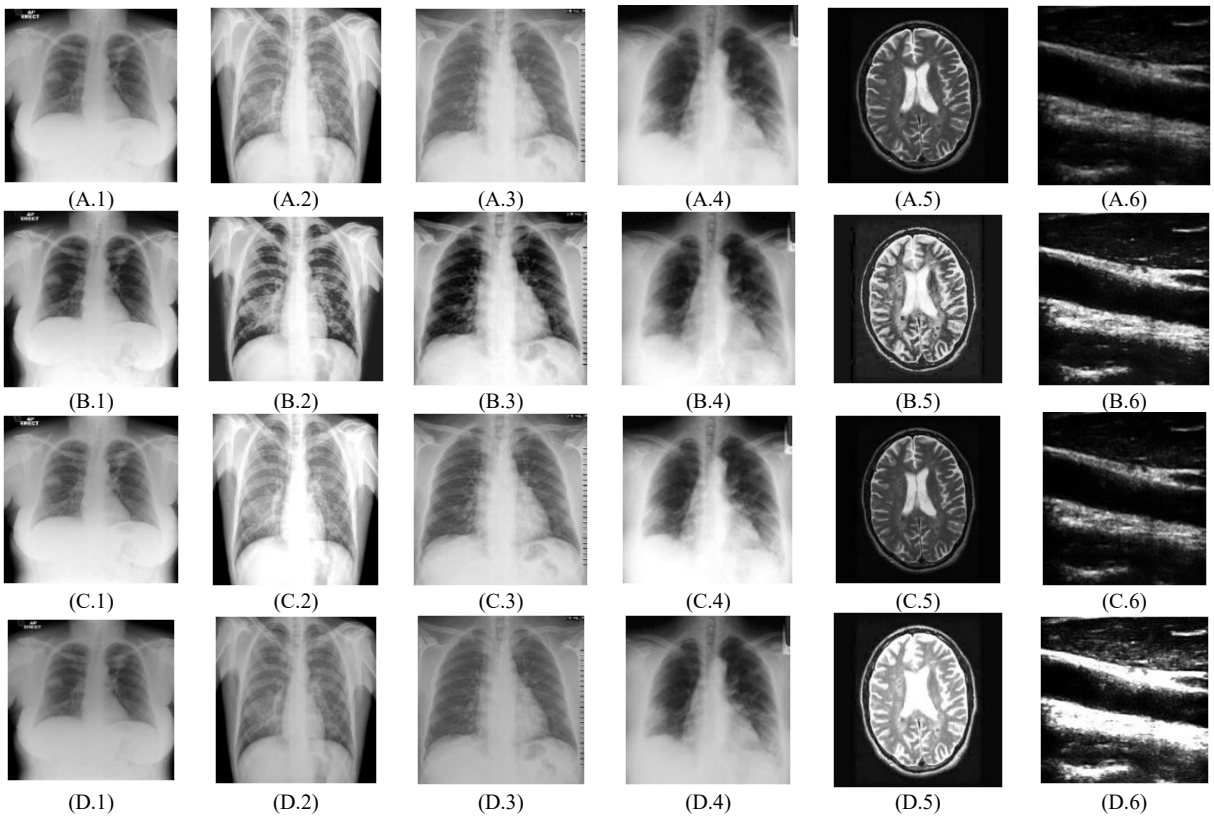

Figure 5. (A.1-A.6) Original medical images, enhanced images using (B.1-B.6) BBHE, (C.1-C.6) TCDHE_SF and (D.1-D.6) DWT_SVD.

MOS: It is a method for qualitative assessment of enhanced images by evaluating their visual clarity. The MOS is a measure of human vision. A MOS score is in the range $[1, 5]$with 1 being the lowest quality and 5 representing the best image. The results shown in **Figure 7** represent the average scores assigned by six experts, who include lab technicians and medical professionals, based on six medical images from different modalities. All images produced using the proposed method achieved an acceptable Mean Opinion Score (MOS) above the threshold. This method effectively preserves the brightness of the images while enhancing them, resulting in minimal visual artifacts.

Although Mean Opinion Score (MOS) evaluations from medical professionals provide valuable perceptual assessment of image quality, they do not directly establish clinical utility in diagnostic tasks. The present study focuses on image enhancement performance rather than task-based clinical validation (e.g., lesion detectability, fracture visibility, or diagnostic accuracy). Comprehensive clinical evaluation remains outside the scope of this work and represents an important direction for further research.

Table 8. Average values of performance metrics computed for various methods.

Methods	AMBE	GMSD	PSNR	SSIM	Original entropy	Enhanced entropy	REC
DWT_SVD	43.68±19.23	0.27±0.09	14.09±6.45	0.71±0.22	5.98±1.17	6.15±1.16	0.86±0.11
HE	75.75±43.19	0.32±0.03	10.88±5.06	0.44±0.29	5.98±1.17	4.91±4.91	0.89±0.09
TCDHE_SF	7.44±6.86	0.18±0.06	29.86±7.07	0.96±0.03	5.98±1.17	5.92±1.21	0.96±0.05
BBHE	24.98±13.11	0.25±0.05	16.67±4.21	0.59±0.22	5.98±1.17	5.71±1.25	0.87±0.09
CLAHE	19.87±10.70	0.24±0.02	17.78±2.23	0.61±0.17	5.98±1.17	**6.60±1.11**	0.91±0.06
MT_PSO	13.94±7.50	0.27±0.07	18.96±2.34	0.87±0.04	5.98±1.17	5.69±1.31	1.11±0.07
Proposed	**4.08±5.42**	**0.13±0.04**	**37.67±8.53**	**0.99±0.01**	5.98±1.17	**5.98±1.16**	**0.99±0.02**

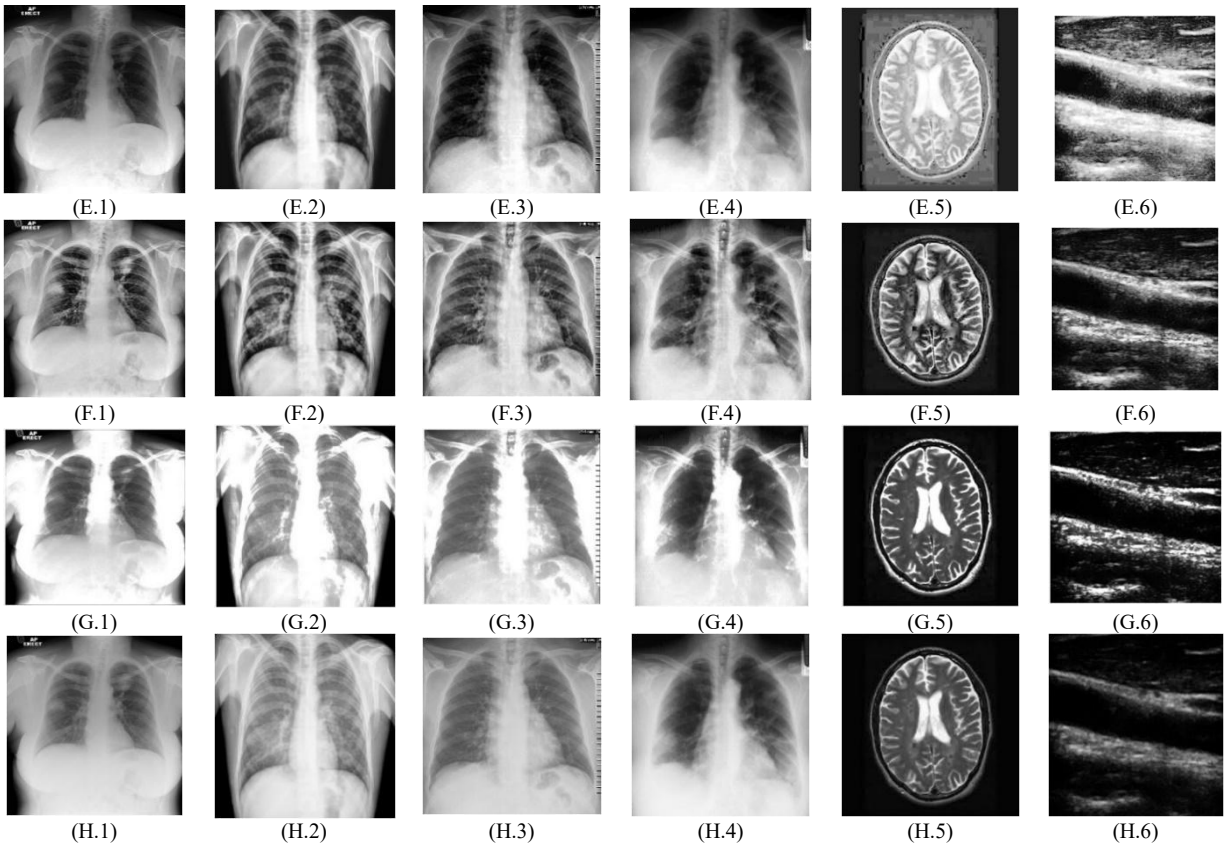

Figure 6. Enhanced images using (E.1-E.6) HE, (F.1-F.6) CLAHE, (G.1-G.6) MT_PSO and (H.1-H.6) the proposed method.

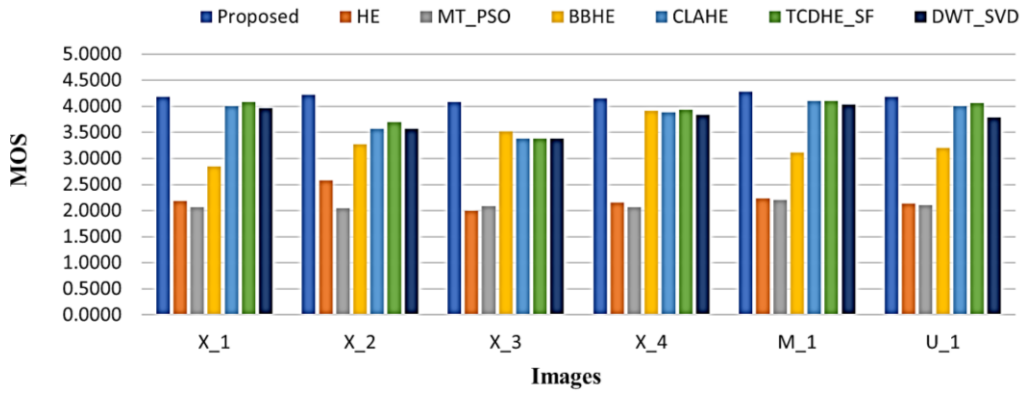

Figure 7. Mean opinion score computed for various methods.

6. Conclusions

Image contrast plays a crucial role in enhancing visual perception across computer vision, medical image processing, pattern recognition, and digital image handling. In recent years, medical image processing has advanced, enabling better diagnosis across related medical modalities. The proposed method is designed to

improve the quality of medical images, providing greater clarity in medical scans. This would help medical experts and doctors correctly identify and provide the best treatment for the disease.

The proposed method is based on a fusion approach that incorporates HE, DWT, and SF. The effectiveness of the proposed method has been evaluated using seven performance metrics: AMBE, SSIM, GMSD, REC, PSNR, and entropy. The experimental results clearly demonstrate that AMBE (4.08), SSIM (0.99), PSNR (37.67 dB), and GMSD (0.13) are the best among state-of-the-art methods. However, the results for REC and entropy are comparable to those of state-of-the-art methods. Also, the average values of all the performance parameters have been computed for three categories of medical datasets to demonstrate the versatility of the proposed method.

To evaluate the efficiency of the proposed enhancement method and traditional methods, a dataset consisting of 150 images is used (across three modalities). While traditional methods seem effective with this small dataset, deep learning approaches typically require significantly larger datasets to achieve higher accuracy. The proposed method specifically targets low-data scenarios where traditional techniques remain practical and computationally efficient. Future research could explore the development of lightweight learning-based models trained on similarly sized datasets, which presents an interesting direction for further work. Additionally, the proposed method can be combined with other image enhancement techniques and further applied to image segmentation.

Conflicts of Interest

All authors declare that they have no conflict of interest.

Acknowledgments

The authors of this manuscript are thankful to the anonymous reviewers for providing their valuable comments. No funding is available for this work. Neha-wrote the manuscript and coding; reviewed the manuscript. Anuj- prepared methodology, debugged the code, and reviewed the manuscript. All the images are acquired from an online repository and are properly cited in the references. No ethical approval is required. Data can be downloaded from an online repository, as cited in the paper.

AI Disclosure

During the preparation of this work the author(s) used generative AI in order to improve the language of the article. After using this tool/service, the author(s) reviewed and edited the content as needed and take(s) full responsibility for the content of the publication.

References

Ahmad, M.S.Z., Ab. Aziz, N.A., Lim, H.S., Ghazali, A.K., & Latiff, A.A. (2025). Impact of image enhancement using contrast-limited adaptive histogram equalization (CLAHE), anisotropic diffusion, and histogram equalization on spine X-ray segmentation with U-net, mask R-CNN, and transfer learning. *Algorithms*, *18*(12), 796. https://doi.org/10.3390/a18120796

Aosiman, A., Abulijiang, A., Abulikemu, A., Abdukirim, T., & Maimaiti, M. (2020). Medical image enhancement algorithm based on histogram equalization and dyadic wavelet transform. In *Proceedings of the 2020 3rd International Conference on Computer Science and Software Engineering* (pp. 181-185). Association for Computing Machinery. New York, USA. https://doi.org/10.1145/3403746.3403925

Atta, R., & Abdel-Kader, R.F. (2015). Brightness preserving based on singular value decomposition for image contrast enhancement. *Optik*, *126*(7-8), 799-803. https://doi.org/10.1016/j.ijleo.2015.02.025

Chandra, N., & Bhardwaj, A. (2024). Medical image enhancement using modified type II fuzzy membership function generated by Hamacher T-conorm. *Soft Computing, 28*(9), 6753-6774. https://doi.org/10.1007/s00500-023-09535-5

Chaudhary, S., Bhardwaj, A., & Rana, P. (2022). Image enhancement by linear regression algorithm and sub histogram equalization. *Multimedia Tools and Applications, 81*, 29919-29938. https://doi.org/10.1007/s11042-022-12830-2

Demirel, H., Ozcinar, C., & Anbarjafari, G. (2010). Satellite image contrast enhancement using discrete wavelet transform and singular value decomposition. *IEEE Geoscience and Remote Sensing Letters*, *7*(2), 333-337. https://doi.org/10.1109/LGRS.2009.2034873

Dougherty, G. (2009). *Digital image processing for medical applications*. Cambridge University Press, UK.

Fu, X., Wang, J., Zeng, D., Huang, Y., & Ding, X. (2015). Remote sensing image enhancement using regularized-histogram equalization and DCT. *IEEE Geoscience and Remote Sensing Letters*, *12*(11), 2301-2305. https://doi.org/10.1109/LGRS.2015.2473164

Gandhamal, A., Talbar, S., Gajre, S., Hani, A.F.M., & Kumar, D. (2017). Local grey level S-curve transformation - a generalized contrast enhancement technique for medical images. *Computers in Biology and Medicine*, *83*, 120-133. https://doi.org/10.1016/j.compbiomed.2017.03.001

Jinju, J., Santhi, N., Ramar, K., & Bama, B.S. (2019). Spatial frequency discrete wavelet transform image fusion technique for remote sensing applications. *Engineering Science and Technology, an International Journal*, *22*(3), 715-736. https://doi.org/10.1016/j.jestch.2019.01.004

Joseph, J., & Periyasamy, R. (2018). A fully customized enhancement scheme for controlling brightness error and contrast in magnetic resonance images. *Biomedical Signal Processing and Control*, *39*, 271-283. https://doi.org/10.1016/j.bspc.2017.08.003

Kahlessenane, F., Khaldi, A., Kafi, R., & Euschi, S. (2021). A DWT based watermarking approach for medical image protection. *Journal of Ambient Intelligence and Humanized Computing*, *12*(2), 2931-2938. https://doi.org/10.1007/s12652-020-02450-9

Kallel, F., & Ben Hamida, A. (2017). A new adaptive gamma correction based algorithm using DWT-SVD for non-contrast CT image enhancement. *IEEE Transactions on NanoBioscience*, *16*(8), 666-675. https://doi.org/10.1109/TNB.2017.2771350

Kim, Y.-T. (1997). Contrast enhancement using brightness preserving bi-histogram equalization. *IEEE Transactions on Consumer Electronics*, *43*(1), 1-8. https://doi.org/10.1109/30.580378

Kumar, S., Bhandari, A.K., Raj, A., & Swaraj, K. (2021). Triple clipped histogram-based medical image enhancement using spatial frequency. *IEEE Transactions on NanoBioscience*, *20*(3), 278-286. https://doi.org/10.1109/TNB.2021.3064077

Liu, K., & Tian, Y. (2020). Research and analysis of deep learning image enhancement algorithm based on fractional differential. *Chaos, Solitons & Fractals*, *131*, 109507. https://doi.org/10.1016/j.chaos.2019.109507

Masters, B.R., Gonzalez, R.C., & Woods, R.E. (2009). Book review: digital image processing, third edition. *Journal of Biomedical Optics*, *14*(2), 029901. https://doi.org/10.1117/1.3115362

Ooi, C.H., Pik Kong, N.S., & Ibrahim, H. (2009). Bi-histogram equalization with a plateau limit for digital image enhancement. *IEEE Transactions on Consumer Electronics*, *55*(4), 2072-2080. https://doi.org/10.1109/TCE.2009.5373771

Panetta, K., K.M.S.K., Rao, S.P., & Agaian, S.S. (2023). Deep perceptual image enhancement network for exposure restoration. *IEEE Transactions on Cybernetics*, *53*(7), 4718-4731. https://doi.org/10.1109/TCYB.2021.3140202

Rao, B.S. (2020). Dynamic histogram equalization for contrast enhancement for digital images. *Applied Soft Computing*, *89*, 106114. https://doi.org/10.1016/j.asoc.2020.106114

Sahnoun, M., Kallel, F., Dammak, M., Kammoun, O., Mhiri, C., Ben Mahfoudh, K., & Ben Hamida, A. (2019). A modified DWT-SVD algorithm for T1-w brain MR images contrast enhancement. *IRBM*, *40*(4), 235-243. https://doi.org/10.1016/j.irbm.2019.04.007

Saifullah, S., & Dreżewski, R. (2023). Modified histogram equalization for improved CNN medical image segmentation. *Procedia Computer Science*, *225*, 3021-3030. https://doi.org/10.1016/j.procs.2023.10.295

Sandeepa, K.S., Jagadale, B.N., Bhat, J.S., Kumar, R.N., Naagund, M.N., & Panchaxri. (2017). Image contrast enhancement using DWT-SVD based masking technique. In *2017 2nd International Conference on Communication and Electronics Systems* (pp. 581-585). IEEE. Coimbatore, India. https://doi.org/10.1109/CESYS.2017.8321144

Sazak, Ç., Nelson, C.J., & Obara, B. (2019). The multiscale bowler-hat transform for blood vessel enhancement in retinal images. *Pattern Recognition*, *88*, 739-750. https://doi.org/10.1016/j.patcog.2018.10.011

Shaout, A., & Han, J. (2023). A novel retinal image contrast enhancement-fuzzy-based method. In *2023 24th International Arab Conference on Information Technology* (pp. 1-6). IEEE. Ajman, United Arab Emirates. https://doi.org/10.1109/ACIT58888.2023.10453851

Singh, N., & Bhandari, A.K. (2021). Principal component analysis-based low-light image enhancement using reflection model. *IEEE Transactions on Instrumentation and Measurement*, *70*, 1-10. https://doi.org/10.1109/TIM.2021.3096266

Sugamya, K., Pabboju, S., & VinayaBabu, A. (2016). Image enhancement using singular value decomposition. In *2016 International Conference on Research Advances in Integrated Navigation Systems* (pp. 1-5). IEEE. Bangalore, India. https://doi.org/10.1109/RAINS.2016.7764388

Tang, J.R., & Mat Isa, N.A. (2017). Bi-histogram equalization using modified histogram bins. *Applied Soft Computing*, *55*, 31-43. https://doi.org/10.1016/j.asoc.2017.01.053

Veluchamy, M., & Subramani, B. (2019). Image contrast and color enhancement using adaptive gamma correction and histogram equalization. *Optik*, *183*, 329-337. https://doi.org/10.1016/j.ijleo.2019.02.054

Wadhwa, A., & Bhardwaj, A. (2020). Enhancement of MRI images of brain tumor using Gr$\ddot {u}$nwald letnikov fractional differential mask. *Multimedia Tools and Applications*, *79*(35), 25379-25402. https://doi.org/10.1007/s11042-020-09177-x

Wadhwa, A., & Bhardwaj, A. (2021). Contrast enhancement of MRI images using morphological transforms and PSO. *Multimedia Tools and Applications*, *80*(14), 21595-21613. https://doi.org/10.1007/s11042-021-10743-0

Wang, Y., Chen, Q., & Zhang, B. (1999). Image enhancement based on equal area dualistic sub-image histogram equalization method. *IEEE Transactions on Consumer Electronics*, *45*(1), 68-75. https://doi.org/10.1109/30.754419

Xue, W., Zhang, L., Mou, X., & Bovik, A.C. (2014). Gradient magnitude similarity deviation: a highly efficient perceptual image quality index. *IEEE Transactions on Image Processing*, *23*(2), 684-695. https://doi.org/10.1109/TIP.2013.2293423

Zhou, M., Jin, K., Wang, S., Ye, J., & Qian, D. (2018). Color retinal image enhancement based on luminosity and contrast adjustment. *IEEE Transactions on Biomedical Engineering*, *65*(3), 521-527. https://doi.org/10.1109/TBME.2017.2700627

Zuo, C., Chen, Q., & Sui, X. (2013). Range limited bi-histogram equalization for image contrast enhancement. *Optik*, *124*(5), 425-431. https://doi.org/10.1016/j.ijleo.2011.12.057